

Hydration Dynamics at a Hydrophobic Surface

Abstract:

Water is the universal solvent of life, crucial to the function of all biomolecules. Proteins, membranes, and nucleic acids all have particular structural properties that are driven by the presence of water. The “hydration shell” of three to four water molecules at biological surfaces is thought to be especially relevant for lubricating dynamic interactions, such as the binding of proteins.¹ Here we explore the phenomenon of hydration dynamics—the local diffusion of water near a simplified surface. This is accomplished by a molecular dynamics simulation to measure two-dimensional diffusion coefficients for water molecules bounded by hydrophobic walls. We use an optimized coarse-grained spherical-symmetric model to describe water-water interactions, the Lennard Jones plus Gaussian (LJG) pair potential^{2,3}, and a 9-3 Lennard-Jones potential to treat the hydrophobic barriers as solid walls in contact with a hard sphere fluid. We find an increase of the self-diffusivity D for molecules close to the hydrophobic barriers, and an overall increase in water diffusion between the hydrophobic plates relative to the bulk case.

Discussion:

The behavior of water at interfaces is a key aspect of biological function that is as of yet not well-understood. The local diffusion of water at a surface, or hydration dynamics, plays a vital role in enabling interactions between biological molecules, and is often a function of the complex physical and chemical landscape of the solvated interface. A protein surface, for example, could have a rugged shape as well as an intricate arrangement of hydrophobic and hydrophilic parts that would result in a heterogeneous hydration dynamics landscape. In order to gain insight into the chemical principles that cause retardation of surface water dynamics relative to bulk diffusion, we simplify the complex biological landscape as an infinite hydrophobic wall and measure diffusion coefficients for water molecules within one, two, or three water layers hydrating the surface and compare to the bulk case.

The model used for capturing the complexity of water-water interactions is a simple spherically symmetric Lennard-Jones plus Gaussian (LJG) pair potential, with coarse-grained parameters (ϵ , σ , B , r_0 , Δ) optimized with a relative entropy minimization approach by comparison to fully atomic water models³. The equation was further non-dimensionalized as follows:

$$u^*(r^*) = \frac{u_{LJG}}{\epsilon} = 4 \left[\left(\frac{1}{r^*} \right)^{12} - \left(\frac{1}{r^*} \right)^9 \right] + B^* \exp \left[- \left(\frac{r^* - r_0^*}{\Delta^*} \right) \right] \quad \text{Equation (1)}$$

where $r^* = r/\sigma$, $B^* = B/\epsilon$, $r_0^* = r_0/\sigma$, $\Delta^* = \Delta/\sigma$, with optimized parameters $\epsilon = 20.38$ kJ/mol, and $\sigma = 2.43$ angstroms, for the entropy-minimized model at a density of 1 g/mL and 300 K, close to ambient conditions for water.

The model used to describe the potential between the water molecules and the hydrophobic barrier is a Lennard-Jones 9-3 potential, where the hydrophobic barrier is approximated as a wall of methane molecules interacting with water as a hard sphere fluid:

$$u_{AB}^*(r_{AB}^*) = \frac{u_{LJ}}{\varepsilon_{AB}} = \frac{4\pi}{3} \rho_{AB}^* \left[\frac{1}{15} \left(\frac{1}{r_{AB}^*} \right)^9 - \frac{1}{2} \left(\frac{1}{r_{AB}^*} \right)^3 \right] \quad \text{Equation (2)}$$

where $r_{AB}^* = r/\sigma_{AB}$, and $\rho_{AB}^* = r\sigma_{AB}^3$ (approximated to be one in this work), with Lennard-Jones parameters $\varepsilon_{AB} = 0.8943$ kJ/mol, and $\sigma_{AB} = 2.429$ angstroms, obtained from the Lorentz-Berthelot mixing rules⁴. Because the scaling of this water-wall interaction is different, we can relate the characteristic scales from this equation to those in Equation (1) to obtain the following:

$$u^*(r^*)_{wall} = \frac{\varepsilon_{AB}}{\varepsilon} \left(\frac{\sigma_{AB}}{\sigma} \right)^3 \frac{4\pi}{3} \rho_{AB}^* \left[\frac{1}{15} \left(\frac{\sigma_{AB}}{\sigma} \right)^6 \left(\frac{1}{r^*} \right)^9 - \frac{1}{2} \left(\frac{1}{r^*} \right)^3 \right] \quad \text{Equation (3)}$$

The velocity Verlet algorithm was used to perform MD simulations in the microcanonical ensemble for both the bulk case (no wall), and the case with the hydrophobic boundaries. The time step used was .001 dimensionless time units, and equilibration was performed for 10,000 time steps, twice with velocity rescaling every 10 steps to bring the temperature to 300 K, or dimensionless $T^* = 0.12$. The simulations were run for 100,000 time steps after equilibration. The initial configurations were made from a cubic lattice and random initial velocities were chosen from a Maxwell-Boltzmann distribution and were energy minimized using a conjugate gradient technique. Systems of 216 water molecules were studied, placed in a box of length L such that the dimensionless density is $\rho^* = 0.48$, which corresponds to a 1 g/mL density. For the bulk case, the Lennard-Jones contribution to the potential was cut and shifted at 2.5. The radial distribution function $g(r)$ was calculated to $L/2$ using 500 bins. For the hydrophobic wall case, the wall was placed at the x - z plane (constant y -coordinate), at a $Y = 0.8 * L$ separation centered at the origin, and initial positions were chosen to be a cubic lattice of length $0.8 * Y$. The density distribution of water molecules between the walls was found across the box length L , using 800 bins. 2D diffusion coefficients of water molecules within one, two, and three layers from the hydrophobic surface were calculated by the slope of the mean squared displacement plotted against simulation time. Multiple simulations were run for each case using different random number seeds.

Case 1: Bulk water. For “bulk” spherically-symmetric water, without the hydrophobic walls, the $g(r)$ was calculated, as shown in Figure 1, in which the coordination of waters, or the hydration shell are visible. The dimensionless diffusivity, D_{bulk} , was found using the Einstein relation. For the three-dimensional case, where all coordinates are considered, $D_{bulk} = 12.6 \pm 0.9$, and for the 2D case, where only the x and z coordinates are considered, for comparison to the hydrophobic walls case, $D_{bulk} = 8.43 \pm 0.8$.

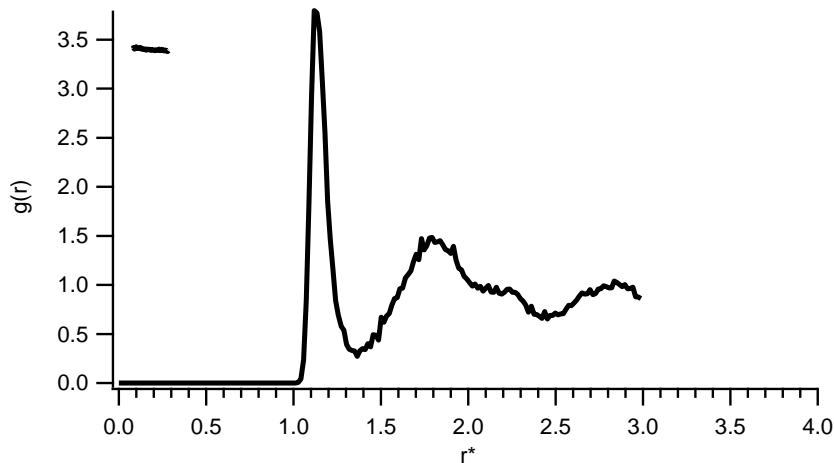


Figure 1: The pair correlation function $g(r)$ for "bulk" water calculated from a MD simulation of the spherically symmetric LJG system. The first and second hydration shells are visible at $r^* = 1.12$ and 1.78 , respectively. Results are similar to in ref. 3

Case 2: Spherically symmetric water between hydrophobic walls. After establishing the self-diffusivities for the bulk case, we turned our attention to the case where there are hydrophobic walls bounding the fluid. In this case, we obtained a density distribution as shown in Figure 2 (note there is a problem with the scaling and the actual numbers do not seem correct for the dimensionless density). The location of the hydrophobic walls, are however visible, in this case at $r^* = 2$ and $r^* = 10$. We see that the water molecules do collect at the surface of the hydrophobic boundaries.

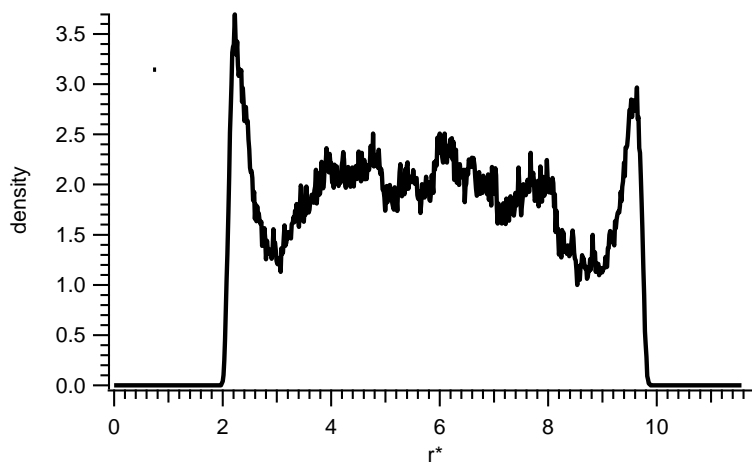


Figure 2: The density distribution for spherically-symmetric water confined between two hydrophobic boundaries, seen at $r^* = 2$ and $r^* = 10$.

The mean squared displacements calculated from molecules "tagged" at each hydration layer are given in Figure 3, where there is a visible trend that the slope, related to the diffusivity D , decreases for water close to the hydrophobic boundary. This suggests that water speeds up the closer it is to the boundary, which is reminiscent of the hydrophobic effect as it is not energetically favorable for the waters to spend much time close to the wall. However, if all the waters are considered (red trace), we can also see that the diffusivity between the plates is faster relative to the bulk case ($D = 112 \pm 9$, vs. $D_{\text{bulk}} = 8.43 \pm 0.8$), and indeed even faster than for the first hydration waters. This is an indication that what we see for the hydration waters may be an artifact of the overall faster water motion between plates. Also, it is perplexing that for the case we may consider to be similar to bulk, that is the diffusion calculated from all the atom positions, we observe even faster water motion.

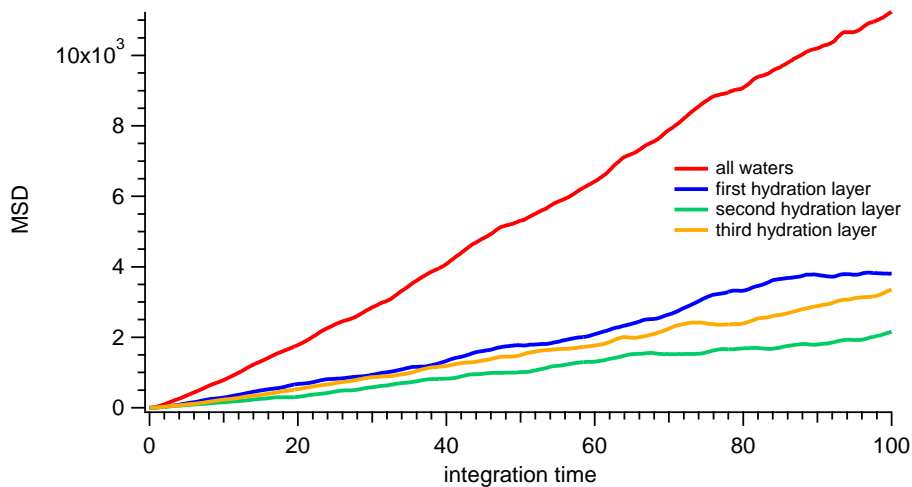


Figure 3: Mean squared displacement for water confined between hydrophobic boundaries.

The values for diffusivity calculated is plotted against distance from the wall in Figure 4, where it is visible that water moves fastest closest to the wall, again providing evidence for the hydrophobic effect.

Conclusion:

We have shown through our simple water model that hydrophobic surfaces may indeed experience faster local water diffusion relative to bulk, which could be one way in which biological surfaces are tuned to interact with water. Although we do observe faster water motion close to the hydrophobic boundary than in the bulk case, there are limitations of the model and the simulation conditions. Since there are problems with the density distribution obtained, there may be a different density within the plates than for the bulk case, which could bias the results. Moving forward, we would have to make sure that the density distribution between the plates is physical, i.e. close to the 1 g/mL, 300 K case. There could also be better ways of finding diffusion coefficients that could be implemented, such as velocity autocorrelation functions.

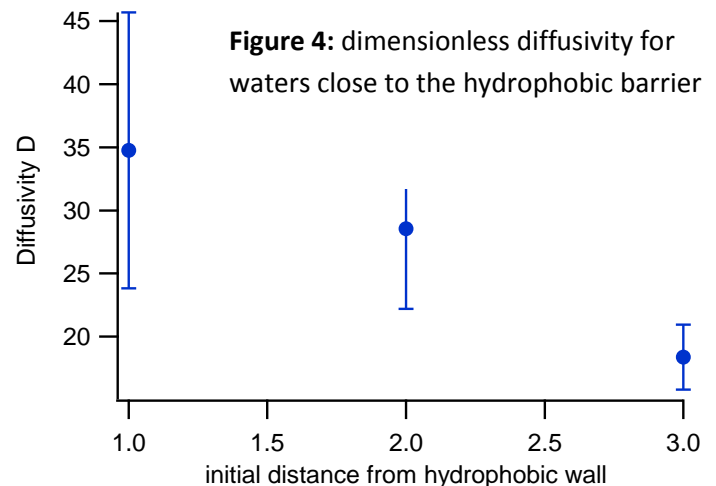


Figure 4: dimensionless diffusivity for waters close to the hydrophobic barrier

Movie Caption: Water diffusing between two hydrophobic barriers.

- (1) Frauenfelder, H.; Fenimore, P. W.; McMahon, B. H. *Biophysical Chemistry* **2002**, *98*, 35-48.
- (2) Cho, C. H.; Singh, S.; Robinson, G. W. *Faraday Discussions* **1996**, *103*, 19-27.
- (3) Chaimovich, A.; Shell, M. S. *Physical Chemistry Chemical Physics* **2009**, *11*, 1901-1915.
- (4) Chaimovich, A.; Shell, M. S. **2012**.

